JACS
JOURNAL OF THE AMERICAN CHEMICAL SOCIETY

Communication

pubs.acs.org/JACS

Quest for Anionic MOF Membranes: Continuous sod-ZMOF Membrane with CO_2 Adsorption-Driven Selectivity

Bassem A. Al-Maythalony,[†] Osama Shekhah,[†] Raja Swaidan,[‡] Youssef Belmabkhout,[†] Ingo Pinnau,[‡] and Mohamed Eddaoudi*[,†]

[†]Functional Materials Design, Discovery & Development Research Group (FMD[3]), Advanced Membranes & Porous Materials Center (AMPMC), Division of Physical Sciences and Engineering (PSE), 4700 King Abdullah University of Science and Technology (KAUST), Thuwal 23955-6900, Kingdom of Saudi Arabia

[‡]Advanced Membranes & Porous Materials Center (AMPMC), Division of Physical Sciences and Engineering, 4700 King Abdullah University of Science and Technology (KAUST), Thuwal 23955-6900, Kingdom of Saudi Arabia

Supporting Information

ABSTRACT: We report the fabrication of the first continuous zeolite-like metal−organic framework (ZMOF) thin-film membrane. A pure phase **sod**-ZMOF, sodalite topology, membrane was grown and supported on a porous alumina substrate using a solvothermal crystallization method. The absence of pinhole defects in the film was confirmed and supported by the occurrence of quantifiable time-lags, for all studied gases, during constant volume/variable pressure permeation tests. For both pure and mixed gas feeds, the **sod**-ZMOF-1 membrane exhibits favorable permeation selectivity toward carbon dioxide over relevant industrial gases such as H_2, N_2, and CH_4, and it is mainly governed by favorable CO_2 adsorption.

Metal−organic frameworks (MOFs), a burgeoning class of functional solid state materials, offer great promise for carbon dioxide capture and separation; particularly from H_2, N_2, and CH_4 containing gases using mainly equilibrium and kinetics based adsorption technologies.[1] MOFs, in the form of microcrystalline powder materials, have found their way into many applications, like gas storage, gas separation, catalysis, and drug delivery,[2] due to their unparalleled large surface areas, structured pore surface functionalization, and prospective tailored small pore windows that can selectively regulate the passing of guest molecules.[3]

The quest for integrating MOFs into film-based applications like gas sensing, membrane-based separations is ever growing and has attracted increasing attention in the past decade.[2,4] This aforementioned interest is directly correlated to the unique structural characteristics and properties of MOFs over conventional porous solids, i.e., (i) the MOF synthesis under mild reaction conditions, (ii) the ability to target and construct a given MOF using the molecular building block approach, (iii) the potential to control and tune the pore window and cage size and functionality, and (iv) the recently proven chemical and thermal stability.[5] Accordingly, our group among others are exploring various strategies for the fabrication of continuous thin-film MOF membranes and their prospective use as an alternative to existing energy-intensive gas separations. Noticeably, it is timely to embark in this emergent research aiming to develop less energy intensive CO_2 removal alternatives such as membrane-based separation, preferably with a favorable permeation of the minor component (i.e., CO_2) in a given gas mixture such as CO_2/CH_4 and CO_2 /H_2 relevant to natural gas upgrading and shifted syngas, respectively.

The main advantages of this emerging technology for gas separations versus conventional sorbent-based separation processes are the relatively lower energy cost, smaller footprint, and modular design.[6] The implementation of MOF membranes for gas purification and separation is in its infancy and is mainly hindered by the persisting challenge to successfully fabricate robust, continuous, and pinhole-free MOF thin-films with very good attachment to the support.[3] This challenge is reflected on the limited number of reports in the open literature pertaining to pure MOFs grown as thin films for gas separation.[3]

Membranes based on zeolitic imidazolate frameworks (ZIFs), a subfamily of MOFs, were reported to show good separation performances with gas permeation selectivities exceeding the limit of Knudsen mechanism behavior.[7] ZIF-7,[7a] ZIF-8,[7b,c] and ZIF-22[7a] membranes showed H_2/CO_2 permeation selectivity (toward H_2) of 13.6, 4.5, and 8.5, respectively, and particularly at relatively high temperatures.

Recently, H_2/CO_2 permeation selectivity of 7.3 was reported for ZIF-90 membrane. This observed molecular sieving driven selectivity is reported to be enhanced to 62.3 upon post-functionalization of ZIF-90 membrane with free aldehyde groups.[8] It is worth noting that an anionic Bio-MOF-1 membrane was reported recently to exhibit an ideal CO_2/CH_4 permeation selectivity of 2.6.[7d]

Despite the importance of post- and precombustion carbon capture and natural gas upgrading applications, only a limited number of studies were reported so far on the use of MOF membranes for the separation of CO_2/N_2, CO_2/CH_4, and CO_2/H_2 gas systems. A practical membrane for CO_2 capture from predominately H_2, N_2, and CH_4 containing gases should exhibit a high permeance for CO_2 as compared to other gases in order to concentrate valuable commodities such as CH_4, O_2, and H_2. To the best of our knowledge, the separation permeation selectivity in favor of CO_2 is scarce and rarely reported for MOF membranes, and it was only reported for a $[Cu_2(bza)_4(pyz)]_n$

Received: November 8, 2014
Published: January 12, 2015

DOI: 10.1021/ja511495j
J. Am. Chem. Soc. 2015, 137, 1754−1757

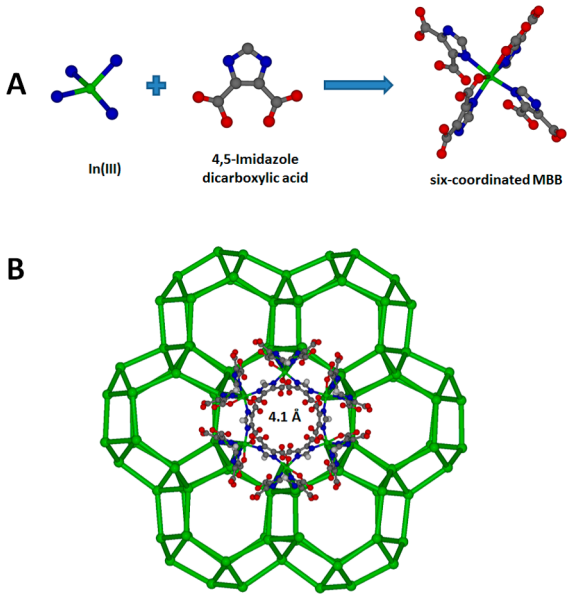

Figure 1. (A) Illustration of the six-coordinated MBB, permitting the requisite rigid and directional tetrahedral building unit, for the construction of the **sod**-ZMOF-1. (B) Projection along the six-membered window of the **sod**-ZMOF-1 showing the diameter of the accessible six membered access to the β-cages. Carbon (gray), indium (green), nitrogen (blue), and oxygen (red).

single crystal MOF membrane.[9] For a more comprehensive account on the performance of different MOF membranes, the reader may refer to reviews by Li et al. and/or Qiu et al.[3]

Herein, we report the fabrication of the first ZMOF membrane with sodalite topology (**sod**-ZMOF). ZMOFs pioneered by our group[10] represent a unique subset of MOFs that are not just topologically related to pure inorganic zeolites but also exhibit distinctive properties: (i) accessible extra-large cavities, (ii) chemical stability, and (iii) cation exchange capability. The anionic character of ZMOFs allows for the tuning of the pore system via extra-framework cations exchange and thus the potential to tune and enhance host−guest interactions toward specific guest molecules. The **sod**-ZMOF-1 is constructed from the assembly of In(III) cations and imidazoledicarboxylate ($ImDC^{2-}$) linkers in the presence of structure directing agents (SDAs) and is formulated as $[In(C_5N_2O_4H_2)_2(C_3N_2H_5)]\cdot(DMF)_x$. The **sod**-ZMOF-1 encompasses large β-cavities accessible via six membered windows. The four membered window has a negligible diameter, and the six membered window has a 4.1 Å diameter (Figure 1). Argon adsorption studies performed on the acetonitrile-exchanged sample of **sod**-ZMOF-1 reveal a reversible Type-I isotherm, indicative of a microporous material with permanent porosity (Figure S1). The apparent BET and Langmuir surface area and pore volume for **sod**-ZMOF-1 were determined to be 474 $m^2 g^{-1}$, 590 $m^2 g^{-1}$, and 0.18 $cm^3 g^{-1}$, respectively. The relatively narrow size of the six-membered window in the **sod**-ZMOF-1 is anticipated to provide selective diffusion and thus allowing a reasonably easy passing of small molecules versus larger ones. In addition, the anionic character of **sod**-ZMOF-1 may alter the adsorption/diffusion, and also in turn permeation properties of given gases, and potentially impacts the gas separation properties of the **sod**-ZMOF-1.

The **sod**-ZMOF-1 membrane was fabricated by slightly adjusting and optimizing the original solvothermal reaction

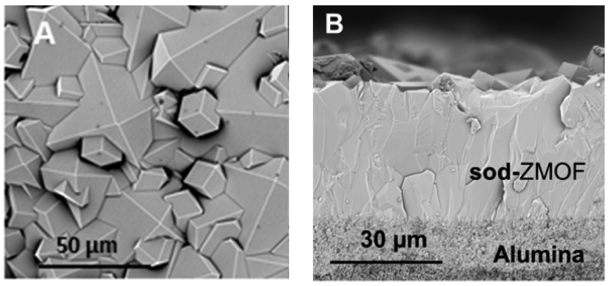

Figure 2. SEM images of **sod**-ZMOF-1 membrane supported on alumina substrate, top view (A) and cross-section (B).

conditions, which permitted the promotion of crystal intergrowth.[10a] After optimizing the fabrication conditions to attach and intergrow **sod**-ZMOF-1 crystals on the porous/activated alumina support, suitable reaction conditions for the fabrication of closed-continuous **sod**-ZMOF-1 thin film were isolated. The successful intergrowth was accomplished by introducing continuous sonication to the adjusted **sod**-ZMOF-1 solvothermal reaction conditions, promoting homogeneous nucleation in the entire reaction mixture. In a 50 mL vial, 4,5-imidazoledicarboxylic acid (0.448 mmol), $In(NO_3)_3\cdot 2H_2O$ (0.145 mmol) in dimethylformamide (DMF) (4.5 mL), CH_3CN (1.5 mL), imidazole (0.666 mL, 1.5 M in DMF), and HNO_3 (1.0 mL, 3.5 M in DMF) were mixed and sonicated until a clear solution was obtained. The alumina substrate was then immersed into solution and the vial was then sealed and heated to 85 °C for 12 h and 105 °C for 23 h. The resultant **sod**-ZMOF-1 film was removed from the reaction mixture and then washed with DMF. Subsequently the DMF guest molecules were exchanged with a low boiling point solvent (acetonitrile) and then the film was dried in open air at room temperature to avoid film cracking during the solvent evaporation process. The powder X-ray diffraction (PXRD) pattern of the **sod**-ZMOF-1 membrane (Figure S2) reveals the successful formation of a pure phase **sod**-ZMOF-1 with a high degree of crystallinity.

The resultant **sod**-ZMOF-1 thin-film membrane with a layer thickness of 35−40 μm, as determined by SEM studies (**sod**-ZMOF-1 SEM images Figure 2), was mounted in a custom-made permeation cell and sealed from both sides with silicon O-rings for leak-tight gas permeation testing. The single gas permeation tests for He, H_2, CO_2, N_2, O_2, CH_4, C_2H_4, and C_2H_6 (>99.99%) gases were performed on the activated **sod**-ZMOF-1 membrane using the constant volume/variable pressure (CV/VP) permeation technique (Schematic S1).[11] To remove any residual guest molecules (mainly acetonitrile) additional activation was performed in situ by evacuation at 308 K. The resultant **sod**-ZMOF-1 membrane was considered to be fully evacuated and activated when the downstream pressure rise was less than 1% during the tightness test. Pure single gas permeation tests were performed by applying an upstream pressure of 2 bar. Successively, the downstream pressure rise was monitored for each single gas permeation run using a 10 Torr transducer. The gas permeation was assumed to be at steady-state when no further variation was observed in the pressure rise, i.e., 7−10 times after the time-lag has elapsed (Figure S3). Interestingly, time lag behavior was observed for all the tested gases (Figure S4) indicating that the film was pinhole-free. The aforementioned film continuity was further supported by the reproducibility of the gas permeation results for various freshly prepared **sod**-ZMOF membranes combined with the elevated O_2/N_2 permeation selectivity, relatively higher than the expected

DOI: 10.1021/ja511495j
J. Am. Chem. Soc. 2015, 137, 1754−1757

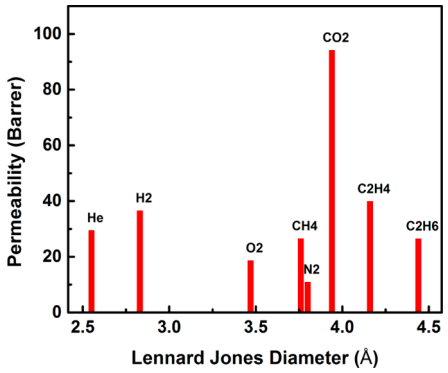

Figure 3. Single gas permeability vs Lennard-Jones diameter of relevant gases (at 308 K) on **sod**-ZMOF-1 membranes.

Knudsen diffusion driven selectivity if the evaluated **sod**-ZMOF membrane was defective (1.7 vs 1.1). Single gas permeation experiments show a sharp maximum in CO_2 permeability compared to all the other tested gases (Table S1). Therefore, as shown in Figure 3, the **sod**-ZMOF-1 membrane exhibits higher ideal permeation selectivity for CO_2 over other evaluated gases. The obtained separation factors for CO_2 over N_2, O_2, and CH_4 were 8.7 (CO_2/N_2), 5.1 (CO_2/O_2), and 3.6 (CO_2/CH_4) (see Table S2), respectively. To further confirm this selective permeation in favor of CO_2, CO_2/CH_4:50/50 (relevant to biogas), and CO_2/N_2:10/90 (relevant to flue gas), gas mixture permeation experiments were carried out using two permeation systems, namely, state-of-the-art CV/VP gas chromatography technique (Schematic S2) and mixture gas permeation combined with continuous gas analysis setup (Schematic S3).

Both experiments revealed a permeation selectivity toward CO_2 of 4 and 10.5 (at 3.4 bar) for the two gases systems, respectively, in good agreement with the ideal permeation selectivity of 3.6 for CO_2/CH_4 and 8.7 for CO_2/N_2, obtained from pure gas permeation tests at 2 bar (Table S4 and Figures S5 and S6). Interestingly for the CO_2−H_2 pair gas system the CO_2 permeability was faster than H_2 with a CO_2/H_2 ideal permeation selectivity of 2.6.

The uncommonly observed reverse-selectivity, for polycrystalline MOF-based membranes,[9] was confirmed by performing CO_2/H_2:30/70 mixture gas permeation (Figure S7) using a continuous gas analysis setup (Schematic S3). Interestingly, the gas mixture experiment reveals a CO_2/H_2 permeation selectivity of 5.2 in favor of CO_2 at 308 K and 3.4 bar. This increase in mixed-gas permeation selectivity compared to ideal permeation selectivity can be attributed to preferential CO_2 adsorption over H_2 in the CO_2/H_2 mixture permeation. To the best of our knowledge, this uncommon selectivity toward CO_2 particularly versus H_2 is the highest reported so far using MOF-based membranes[9] (see Table S3). To confirm this unprecedented adsorption driven permeation selectivity in MOF based membranes, further permeation tests were performed at two additional temperatures, 268 and 353 K, as it was anticipated that such an adsorption-driven behavior will be temperature dependent where the CO_2/H_2 selectivity will decrease with a temperature increase. Indeed, the CO_2/H_2 permeation selectivity of 5.2 at 308 K increased to 12 at lower temperature (268 K) (Figure S8) and decreased to 2.5 at relatively higher temperature (353 K) (Figure S9). The enhanced CO_2/H_2 permeation selectivity with temperature decrease confirms that CO_2/H_2 gas permeation is mainly governed by adsorption. In contrast to ZIFs, which are neutral, the anionic character of ZMOFs with the presence of extra-framework imidazolium cations,[10a] is mainly responsible for the reversed CO_2/H_2 permeation selectivity observed in the **sod**-ZMOF-1 membrane.[12] These unique findings are of prime importance as an economically feasible processing of shifted syngas (CO_2/H_2:30/70 mixture) requires a selective membrane for the less dominant fraction, namely, CO_2. To further assess the impact of the CO_2 adsorption in the **sod**-ZMOF-1 membrane selectivity for various gas mixtures containing CO_2, CO_2 adsorption isotherms were recorded at different temperatures in the low subatmospheric pressures for the **sod**-ZMOF-1 crystalline bulk material (Figure S10a). The CO_2 heat of adsorption (Q_{st}) at low loading was found to be around 29 kJ mol^{-1} (Figure S10b) and supporting the presence of favorable interactions between CO_2 via its quadruple moment and the extra-framework imidazolium cations balancing the charged framework and occupying the **sod**-ZMOF-1 confined pore system. Additionally, the adsorption data for N_2, O_2, CH_4, and H_2 (Figure S11a) revealed a relatively much lower adsorption uptake at room temperature than CO_2. Congruently under these conditions, it is anticipated that **sod**-ZMOF-1 will express favorable and enhanced adsorption selectivity toward CO_2 particularly against H_2 as compared to ZIFs.[7c] Ideal adsorption solution theory (IAST) was employed to derive the CO_2/N_2, CO_2/O_2, CO_2/CH_4, and CO_2/H_2 adsorption selectivities in gas mixtures akin to industrial gases (Figure S11b).[13] The IAST predicted gas adsorption equilibrium selectivity indicates that **sod**-ZMOF-1 exhibits a higher CO_2 adsorption selectivity versus H_2 than for CH_4, N_2, and O_2, i.e., $CO_2/H_2 \gg CO_2/N_2 \approx CO_2/O_2 > CO_2/CH_4$. The observed trend is in accordance with the polarizability of CO_2, promoting its favorable interactions with the anionic framework and its hosted imidazolium cations. Furthermore, the single gas permeation and sorption data were analyzed using the solution-diffusion model, applicable to structures with nominal pore diameter less than 10 Å.[14] In this model, gas permeability through a dense or microporous framework is the product of diffusion and solubility.

Diffusion is characterized by a diffusion coefficient, *D*, which is a measure of the kinetics of gas transport through the membrane (thin film) and can be directly correlated to the gas molecular size. The value of *D* can be derived from experimental permeation time-lags data or back-calculated from the adsorption and permeation data. Solubility is characterized by a sorption coefficient, *S*, which comprises the framework interactions with the gases and can be correlated well with the gas condensability. The value of *S* can be obtained indirectly from the solution-diffusion model via knowledge of *P* and *D* or directly from equilibrium adsorption isotherms if the material density is known (see the Supporting Information).

Here, since independent measurements of both *P* and *S* using gas permeation and adsorption isotherms, respectively, were available, *D* was more accurately calculated as $D = P/S$.[15]

Figure 4a shows that larger gas molecules experience more resistance to diffusion through the **sod**-ZMOF-1 pore system, 4.1 Å pore aperture size, causing a general decline in diffusion coefficients with size (here used as Lennard-Jones diameters).[15] A 20-fold decline in the *D* coefficient is observed to occur from H_2 (2.8 Å) through CO_2 to C_2H_6 (>4 Å). With regards to adsorption at equilibrium, condensable gases exhibit generally stronger interactions in accordance with the anticipated increase in the solubility coefficient, *S*, with the increasing boiling point (Figure 4b). However, in the solution-diffusion model the rate-limiting step in gas permeation is typically Fickian diffusion

DOI: 10.1021/ja511495j
J. Am. Chem. Soc. 2015, 137, 1754−1757

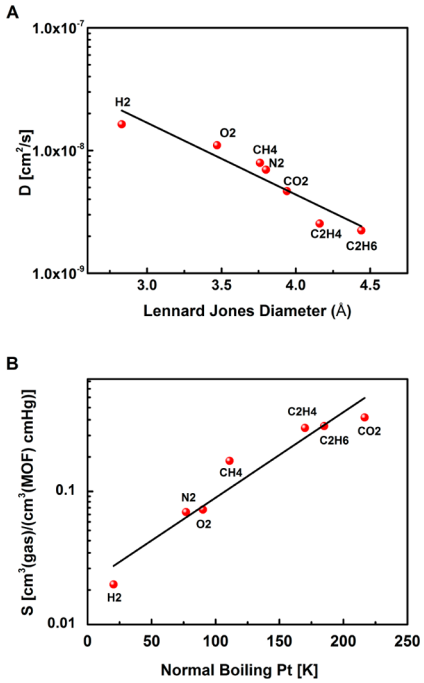

Figure 4. (A) Diffusion coefficients (D) vs Lennard-Jones diameter. (B) Solubility coefficients (S) (from sorption data) vs normal boiling point as determined from CV/VP permeation technique at 2 bar.

across the film thickness.[14] That is, one might expect permeability coefficients to decrease with penetrant size, as is often observed in the case of ZIF-8.[16] Conversely, the **sod**-ZMOF-1 combined permeation and sorption data reveal adsorption-driven permeation that rather trends with the condensability of the gas. Lastly, the key finding is that despite the restriction on the diffusion of CO_2 by the rigid and relatively small pore apertures, the remarkable affinity of **sod**-ZMOF-1 to CO_2, due to the presence of imidazolium cations, grants it the maximum, adsorption-driven, permeability of all tested gases.

In conclusion, we have succeeded, for the first time, to prepare a pinhole-free thin-film ZMOF membrane with a sodalite topology, **sod**-ZMOF-1, using a solvothermal crystallization method. The looked-for crystal intergrowth was achieved by inducing uniform nucleation in the reaction mixture. The **sod**-ZMOF-1 membrane continuity was confirmed by the observed time-lag behavior for all the studied gases as well as by probing the competitive permeation of O_2 and N_2 (largely in favor of O_2). The particular anionic character of the **sod**-ZMOF-1 membrane prone to interactions with the quadruple CO_2 and the small pore window size (4.1 Å) makes it suitable for CO_2 separation and capture applications. This newly reported adsorption driven permeation behavior in favor of CO_2 for polycrystalline MOF membranes, corroborated with analysis of diffusion and sorption behaviors via the solution-diffusion model, can be regarded as a breakthrough finding for the rational design of a MOF membrane targeting CO_2 capture and separation.

The **sod**-ZMOF-1 is certainly a suitable platform toward the fabrication of tunable MOF thin-film membranes for various gas separation applications. Research is in progress to evaluate and assess the impact of various exchanged extra-framework cations, resulting in a post-modified **sod**-ZMOF-1, on the adsorption and permeation properties of various gases relevant to CO_2 capture and light hydrocarbons separation.

■ ASSOCIATED CONTENT

Supporting Information

Experimental details, PXRD, low- and high-pressure gas sorption isotherms, and thin-film permeation studies. This material is available free of charge via the Internet at http://pubs.acs.org.

■ AUTHOR INFORMATION

Corresponding Author

*mohamed.eddaoudi@kaust.edu.sa

Notes

The authors declare no competing financial interest.

■ ACKNOWLEDGMENTS

Research reported in this publication was supported by the King Abdullah University of Science and Technology (KAUST).

■ REFERENCES

(1) (a) Xiang, S.; He, Y.; Zhang, Z.; Wu, H.; Zhou, W.; Krishna, R.; Chen, B. *Nat. Commun.* **2012**, *3*, 954. (b) Nugent, P.; Belmabkhout, Y.; Burd, S. D.; Cairns, A. J.; Luebke, R.; Forrest, K.; Pham, T.; Ma, S.; Space, B.; Wojtas, L. *Nature* **2013**, *495*, 80.

(2) Kuppler, R. J.; Timmons, D. J.; Fang, Q. R.; Li, J. R.; Makal, T. A.; Young, M. D.; Yuan, D. Q.; Zhao, D.; Zhuang, W. J. H.; Zhou, C. *Coord. Chem. Rev.* **2009**, *253*, 3042.

(3) (a) Li, J. R.; Sculley, J.; Zhou, H.-C. *Chem. Rev.* **2012**, *112*, 869. (b) Qiu, S.; Xue, M.; Zhu, G. *Chem. Soc. Rev.* **2014**, *43* (16), 6116−6140.

(4) (a) Shekhah, O.; Liu, J.; Fischer, R. A.; Woell, C. *Chem. Soc. Rev.* **2011**, *40*, 1081. (b) Li, J. R.; Kuppler, R. J.; Zhou, H.-C. *Chem. Soc. Rev.* **2009**, *38*, 1477. (c) Shah, M.; McCarthy, M. C.; Sachdeva, S.; Lee, A. K.; Jeong, H.-K. *Ind. Eng. Chem. Res.* **2012**, *51*, 2179.

(5) (a) Eddaoudi, M.; Li, H. L.; Yaghi, O. M. *J. Am. Chem. Soc.* **2000**, *122*, 1391. (b) Ferey, G. *Chem. Soc. Rev.* **2008**, *37*, 191. (c) Kitagawa, S.; Kitaura, R.; Noro, S. *Angew. Chem., Int. Ed.* **2004**, *43*, 2334.

(6) (a) Freemantle, M. *Chem. Eng. News* **2005**, *83*, 3. (b) Chung, T.-S.; Jiang, L. Y.; Li, Y.; Kulprathipanja, S. *Prog. Polym. Sci.* **2007**, *32*, 483. (c) Koros, W.; Fleming, G. *J. Membr. Sci.* **1993**, *83*, 1−80.

(7) (a) Qiu, S.; Xue, M.; Zhu, G. *Chem. Soc. Rev.* **2014**, *43*, 6116. (b) Bux, H.; Feldhoff, A.; Cravillon, J.; Wiebcke, M.; Li, Y.-S.; Caro, J. *Chem. Mater.* **2011**, *23*, 2262. (c) Shekhah, O.; Swaidan, R.; Belmabkhout, Y.; du Plessis, M.; Jacobs, T.; Barbour, L. J.; Pinnau, I.; Eddaoudi, M. *Chem. Commun.* **2014**, 2089. (d) Bohrman, J. A.; Carreon, M. A. *Chem. Commun.* **2012**, *48*, 5130.

(8) Huang, A.; Wang, N.; Kong, C.; Caro, J. *Angew. Chem., Int. Ed.* **2012**, *51*, 10551.

(9) Takamizawa, S.; Takasaki, Y.; Miyake, R. *J. Am. Chem. Soc.* **2010**, *132*, 2862.

(10) (a) Liu, Y. L.; Kravtsov, V. C.; Larsen, R.; Eddaoudi, M. *Chem. Commun.* **2006**, 1488. (b) Brant, J. A.; Liu, Y. L.; Sava, D. F.; Beauchamp, D.; Eddaoudi, M. *J. Mol. Struct.* **2006**, *796* (1−3), 160−164. (c) Eddaoudi, M.; Sava, D. F.; Eubank, J. F.; Adil, K.; Guillerm, V. *Chem. Soc. Rev.* **2015**, *44*, 228.

(11) Czichos, H.; Saito, T.; Smith, L. *Springer Handbook of Materials Measurement Methods*; Springer: New York, 2006; Vol. 978.

(12) Eubank, J. F.; Mouttaki, H.; Cairns, A. J.; Belmabkhout, Y.; Wojtas, L.; Luebke, R.; Alkordi, M. H.; Eddaoudi, M. *J. Am. Chem. Soc.* **2011**, *133*, 14204.

(13) (a) Chen, H.; Sholl, D. S. *Langmuir* **2007**, *23*, 6431. (b) Myers, A. L.; Prausnitz, J. M. *AIChE* **1965**, *11*, 121.

(14) Baker, R. *Membrane Technology and Applications*; Wiley: New York, 2012.

(15) Yampolskii, Y. P.; Pinnau, I.; Freeman, B. D. *Materials Science of Membranes for Gas and Vapor Separation*; Wiley Online Library: New York, 2006.

(16) Bux, H.; Liang, F.; Li, Y.; Cravillon, J.; Wiebcke, M.; Caro, J. *J. Am. Chem. Soc.* **2009**, *131*, 16000.

DOI: 10.1021/ja511495j
J. Am. Chem. Soc. 2015, 137, 1754−1757